CERN / SPSLC 96-47
SPSLC/P302
October 20, 1996

Antihydrogen Production and Precision Experiments

The ATHENA Collaboration

M. H. Holzscheiter[a1], G. Bendiscioli[b], A. Bertin[c], G. Bollen[d], M. Bruschi[c] C. Cesar[e], M. Charlton[f], M. Corradini[g], D. DePedis[h], M. Doser[d], J. Eades[d] R. Fedele[i], X. Feng[d,*], F. Galluccio[i], T. Goldman[a], J. S. Hangst[j], R. Hayano[k] D. Horváth[d,*], R. J. Hughes[a], N. S. P. King[a], K. Kirsebom[j], H. Knudsen[j] V. Lagomarsino[l], R. Landua[d], G.Laricchia[f], R. A. Lewis[m], E. Lodi-Rizzini[g] G. Manuzio[l], U. Marconi[c], M. R. Masullo[i], J. P. Merrison[j], S. P. Møller[j] G. L. Morgan[a], M. M. Nieto[a], M. Piccinini[c], R. Poggiani[n], A. Rotondi[b], G. Rouleau[d,*] P. Salvini[b], N. Semprini-Cesari[c], G. A. Smith[m], C. M. Surko[o], G. Testera[l], G. Torelli[n] E. Uggerhøj[j], V. G. Vaccaro[i], L. Venturelli[g], A. Vitale[c], E. Widmann[d], T. Yamazaki[k] Y. Yamazaki[k], D. Zanello[h], A. Zoccoli[c]

a. Los Alamos National Laboratory, Los Alamos, New Mexico 87545, U.S.A.
b. Pavia University & INFN , Pavia, Italy
c. Bologna University & INFN, Bologna, Italy
d. CERN, CH1211 Geneva, Switzerland
e. Escola Tecnica Federal do Ceara, Fortaleza, CE 60040-531, Brazil
f. Dept. of Physics & Astronomy, University College London, London, WC1E6BT, UK
g. Brescia University & INFN , Brescia, Italy
h. Rome University "La Sapienza" & INFN , Rome, Italy
i. Napoli University & INFN, Mostra d'Oltremare Pad. 20, I-80125 Napoli, Italy
j. Inst. for Physics & Astronomy, University of Aarhus, DK-8000 Aarhus C, Denmark
k. University of Tokyo, Tokyo, Japan
l. Genoa University & INFN, Via Dodecaneso 33, I-16146 Genoa, Italy
m. Pennsylvania State Univ., 303 Osmond Laboratory, University Park, PA 16802, U.S.A.
n. Pisa University & INFN, I-56100 Pisa, Italy
o. University of California at San Diego, La Jolla, CA 92093-0319, U.S.A.
⋆ visitor at CERN

[1]Spokesperson, Email: holzscheiter@cern.ch

ABSTRACT

The study of CPT invariance with the highest achievable precision in all particle sectors is of fundamental importance for physics. Equally important is the question of the gravitational acceleration of antimatter.

In recent years, impressive progress has been achieved at the Low Energy Antiproton Ring (LEAR) at CERN in capturing antiprotons in specially designed Penning traps, in cooling them to energies of a few milli-electron volts, and in storing them for hours in a small volume of space. Positrons have been accumulated in large numbers in similar traps, and low energy positron or positronium beams have been generated. Finally, steady progress has been made in trapping and cooling neutral atoms.

Thus the ingredients to form antihydrogen at rest are at hand. We propose to investigate the different methods to form antihydrogen at low energy, and to utilize the best of these methods to capture a number of antihydrogen atoms sufficient for spectroscopic studies in a magnetostatic trap.

Once antihydrogen atoms have been captured at low energy, spectroscopic methods can be applied to interrogate their atomic structure with extremely high precision and compare it to its normal matter counterpart, the hydrogen atom. Especially the 1S-2S transition, with a lifetime of the excited state of 122 msec and thereby a natural linewidth of 5 parts in 10^{16}, offers in principle the possibility to directly compare matter and antimatter properties at a level of 1 part in 10^{18}. Such precision can only be achieved once the antihydrogen atoms have been cooled to milli-Kelvin energies, which should be achievable with a combination of laser cooling followed by adiabatic cooling.

In the first phase of the experiment we will study the formation rates of antihydrogen atoms and their capture in a magnetic gradient trap, by observing the annihilation of antihydrogen atoms impinging on the surrounding walls of the experiment with an appropriate detector. At this stage, working with atoms at about 1 K temperature, direct tests of CPT conservation of the electromagnetic interaction at a level of 1 part in 10^{10} and better by 1S-2S two-photon spectroscopy appear feasible. In the second phase we will cool the stored antihydrogen atoms using laser cooling methods similar to those used for hydrogen spectroscopy followed by adiabatic cooling and then investigate the atomic structure of antihydrogen using Doppler-free two-photon spectroscopic techniques. Additionally, comparison of the gravitational masses of hydrogen and antihydrogen, using either ballistic or spectroscopic methods, can provide direct experimental tests of the Weak Equivalence Principle for antimatter at a high precision.

1 Introduction

CPT invariance is a fundamental property of quantum field theories in flat space-time, which results from the basic requirements of locality, Lorentz invariance and unitarity [1–5]. Principal consequences include the predictions that particles and their antiparticles have equal masses and lifetimes, and equal and opposite electric charges and magnetic moments. It also follows that the fine structure, hyperfine structure, and Lamb shifts of matter and antimatter bound systems should be identical.

A number of experiments have tested some of these predictions with impressive accuracy [6], e.g. with a precision of 10^{-12} for the difference between the moduli of the magnetic moment of the positron and the electron [7] and of 10^{-9} for the difference between the proton and antiproton charge-to-mass ratio [8]. However, the most stringent CPT test comes from a mass comparison of neutral kaon and antikaon, where the tremendous accuracy of 10^{-18} has been reached, albeit in a theoretically dependent manner.

Such a fundamental theorem must, of course, be tested as stringently as possible wherever feasible. In this regard, one may draw an analogy to M. Goldhaber's initial tests of baryon number violation, which is now understood to be by no means as significantly deep a principle as CPT. And indeed, pursuit of more vigorous tests of the baryon conservation law was not forthcoming before a theoretical context (Grand Unification) for its possible violation had been established. CPT violation is now on the threshold of a similar transition: from clearly important but with no concept of specific implications of its violation; to a deeper understanding of the significance, importance and physical mechanism for its violation [9–20].

The suggestion of CPT violation is of course controversial, despite the fact that the conservation theorem has only been proven in flat space-time [21]. However, the suggestion follows the classic pattern of P and CP violation, or baryon number violation by supersymmetry: It connects what previously seemed inviolable to interactions which have never previously been fully understood. Although the matter is not settled in the latter case, the example of the former two, as well as the recent theoretical advances linking CPT violation to the deeply fundamental questions of gravity and superstrings, makes it imperative to begin at once to increase the seriousness with which this question is attacked experimentally.

The availability of antihydrogen atoms produced and stored at very low energies would offer new possibilities for a very precise comparison of matter and antimatter systems. In particular, the long lifetime (122 ms) of the metastable 2S level sets an ultimate limit for measuring the 1S-2S energy difference of 10^{-18}, if the line width can be reduced to the quantum limit [22], and if the centre of the spectral line is determined to one part in 10^3. For a more detailed discussion of these and related issues, see also ref. [23]. These limits can only be reached by cooling antihydrogen to the lowest possible temperatures, which are in the milli-Kelvin range if laser cooling is used.

Any difference e.g. in the frequency of the 1S-2S transition would signal new physics. Such an exciting result may be due to CPT violation, but it could also stem from an anomalous red-shift because of a different gravitational interaction of matter and antimatter [24]. A continuous observation of such a difference over the solar period would test such a possibility at a level of accuracy of 10^{-8}, if the range of the anomalous gravitational interaction would be larger than the distance between the Earth and the Sun, but smaller than the size of our galaxy.

As a long term goal, a direct comparison of the gravitational acceleration of hydrogen and antihydrogen in the Earth's gravitational field can be envisaged. Once the technique of cooling antihydrogen to the Dopper limit (3 mK) has been demonstrated, such ballistic measurements will become possible, albeit with a more moderate precision.

2 Experimental overview

Using the method developed at LEAR [8, 25], antiprotons can be captured in an electromagnetic field configuration known as a Penning trap, and cooled to sub-eV temperatures by electron cooling. We plan to accumulate 10^7 cold antiprotons from the Antiproton Decelerator (AD) [26] proposed at CERN in such a trap enclosed in a large diameter superconducting magnet.

Large numbers of positrons have been accumulated in similar field configurations. Our collaboration plans to use a system based upon the positron accumulator presently operated at the University of California in San Diego, in which 10^8 low energy positrons are routinely accumulated in a few minutes. One major modification described below is the addition of a final ultra-high vacuum section which will be separated by fast valves, both from the main accumulator and from the antihydrogen experiment, to store the positrons until needed for the recombination.

One of the major challenges will consist of bringing the antiprotons and positrons in close contact for a time sufficiently long to allow the recombination process to take place. To combine free positrons with the antiprotons it has been proposed to use nested Penning traps [27, 28], a combined RF/Penning trap configuration [29], or to inject a (pulsed or continuous) beam of low energy positronium atoms into stored antiprotons [30].

In the nested traps the oppositely charged antiprotons and positrons are stored in two different potential wells in close proximity and are cooled to low energy. At the time of recombination these two clouds need to be merged while preserving their low temperature and high densities. While the theoretical rate for this process is attractively high, this method may present a number of serious challenges, and despite a number of experimental efforts, no recombination of electrons and protons into hydrogen has been observed to date.

In a combined radio-frequency (Paul) and Penning trap particles of opposite electric charge can be confined by using the Penning trap for one species (i.e. the proton) and the superimposed RF fields to store the other particle (i.e. the electrons). Such a trap has recently been demonstrated to hold electrons and protons for long times, but the main problem identified was the heating of the particles by the RF fields, prohibiting high densities and low temperatures, both essential ingredients for efficient recombination and subsequent confinement of the neutrals.

In both these methods the recombination trap can be loaded with positrons by injecting an intense pulse from an external positron accumulator. These positrons are then recaptured and cooled by synchrotron radiation to the ambient temperature of the system.

A third possibility to form antihydrogen consists of bringing the positron to the antiproton in the form of a neutral positronium atom. Here positrons injected into the recombination region as a beam would be converted into positronium atoms in close proximity to the trapped antiprotons. In this scenario accumulation in an external positron trap may be used to enhance the instantaneous intensity of the positron beam used for positronium generation in the trap to allow for better background discrimination.

Once antiprotons and positrons have been recombined, the confinement by the electric forces ceases and the antihydrogen atoms would escape, hit the nearest wall, and annihilate. To confine the produced antihydrogen atoms magnetic gradients interacting with their magnetic moment can be used. This requires superimposing a strong magnetic gradient field onto the constant field necessary for the Penning trap. Typically a combination of quadrupole coils (Ioffe bars) for radial confinement and Helmholtz coils for the axial confinement is used [31].

We plan to use a large diameter, cold bore, superconducting magnet to house the antiproton trap, the positron storage trap, and the actual recombination trap inside a completely sealed, cryogenic vacuum environment. These components will be located inside a separate vacuum system, which can be inserted and removed from the main solenoid without affecting its cryogenic performance, and which can be cooled to a temperature at or below 0.5 K using a ^{3}He dilution (or evaporative) refrigerator.

The magnet coils to superimpose the Ioffe-Pritchard-type trap [32] onto the homogeneous field will be mounted on the inside of the main solenoid, and will be thermally coupled to the main cryogenic bath. The well depth of the magnetic trap has been designed such that a significant fraction of the formed antihydrogen can be confined.

This system will provide the flexibility needed to investigate several different recombination methods, in particular the (stimulated) radiative recombination in nested or combined traps (see section 5.3 and 5.4) and the positronium reaction (see section 5.5). The necessary detectors to study the formation and subsequent annihilation of antihydrogen as a function of time after the injection of positrons and antiprotons, and also as a function of trap parameters (well depths of antiproton/positron traps, density of charged particle clouds, magnetic well depth, etc.) will be mounted in the space between the inner vacuum shell and the Ioffe-Pritchard trap coils. Finally, access is provided for laser beams to the neutral trap (for stimulated recombination, laser cooling, and for spectroscopy), and the space for a 121.5 nm photon detector to observe the 2P-1S fluorescence is foreseen.

Figure 1 shows a general lay-out of the central portion of the apparatus containing the antiproton capture trap, the recombination trap with superimposed neutral trap and detector system, and the final positron storage trap. These individual items will be discussed in more detail in the subsequent chapters. The initial goal of our collaboration (see chapter 9) is to reproduce the precision demonstrated in hydrogen by the groups at MIT and the MPI Munich. Such a precision can be achieved with the system as described here and $\approx$ 1000 Atoms at 0.5 K in the magnetic trap.

3 Capture and cooling of antiprotons

3.1 Current Status

The technique of capturing antiprotons into traps and cooling them to milli-eV energies has been developed at LEAR over the last 10 years [33, 34]. The antiproton beam from LEAR, with 5.9 MeV kinetic energy, is degraded by a carefully optimized system of entrance counters and foils. To minimize longitudinal emittance growth and angular straggling, the material for the different beam monitors and windows is carefully chosen such that the major energy loss only occurs in the final (degrading) foil, which is part of the trap structure. The fraction of antiprotons exiting this last foil with energies in the 10-30 keV range (typically $\sim$ 1 - 2% [35]) can then be dynamically captured in a multi-ring Penning trap. This is achieved by applying first a reflective voltage at the downstream electrode of the Penning trap, and then - before the reflected antiprotons leave the trap through the entrance electrode - rapidly ramping up to the full capture voltage. The pulse length from LEAR together with the desired energy to be captured dictate the length of the trap structure. In PS200 this length is 50 cm.

The trap structure consists typically of seven electrodes: the entrance foil, a central region comprising five cylinders (two endcaps, two compensation electrodes, and the central ring), and a cylindrical high voltage exit electrode. The trap system is situated in the cryogenic bore of a superconducting solenoid capable of generating a magnetic field of 3 or 6 Tesla. The geometry of the central trap system is carefully chosen to produce a harmonic, orthogonalized quadrupole potential in the central region [36]. Its purpose is twofold: initially to store cold electrons, and then to collect the cooled antiprotons. Two experiments at LEAR have demonstrated trapping and cooling of antiprotons to sub-eV energies. PS 196 is using a small trap system of L =12 cm length and D = 1.2 cm diameter, and a capture voltage $U_c \approx 3$ kV. The dimensions are optimized for having precise control of the harmonic properties of the Penning trap, but the small trap size results in a capture efficiency of only 10^{-4}. The PS 200 system (L = 50 cm, D = 3.8 cm, $U_c \leq 30$ kV) is designed to capture the largest possible number of antiprotons in this energy regime. Capture efficiencies of typically 0.5% are achieved, resulting in the capture of more than 10^6 antiprotons from a single LEAR bunch.

The initial kinetic energy of antiprotons after capture is in the keV range. Electron cooling is used to reduce the antiproton energy to values below 1 meV. For this purpose, a dense electron cloud (in PS200 $\sim 10^9$ electrons are used) is preloaded into the central region of the trap. These electrons cool to equilibrium with their cryogenic environment via synchrotron radiation, with a time constant of 0.4 s at 3 Tesla. The antiprotons oscillate through the cold electron cloud and loose their energy via Coulomb collisions with a time constant of a few minutes. The efficiency observed for this process is better than 90% in both experiments. Owing to the very

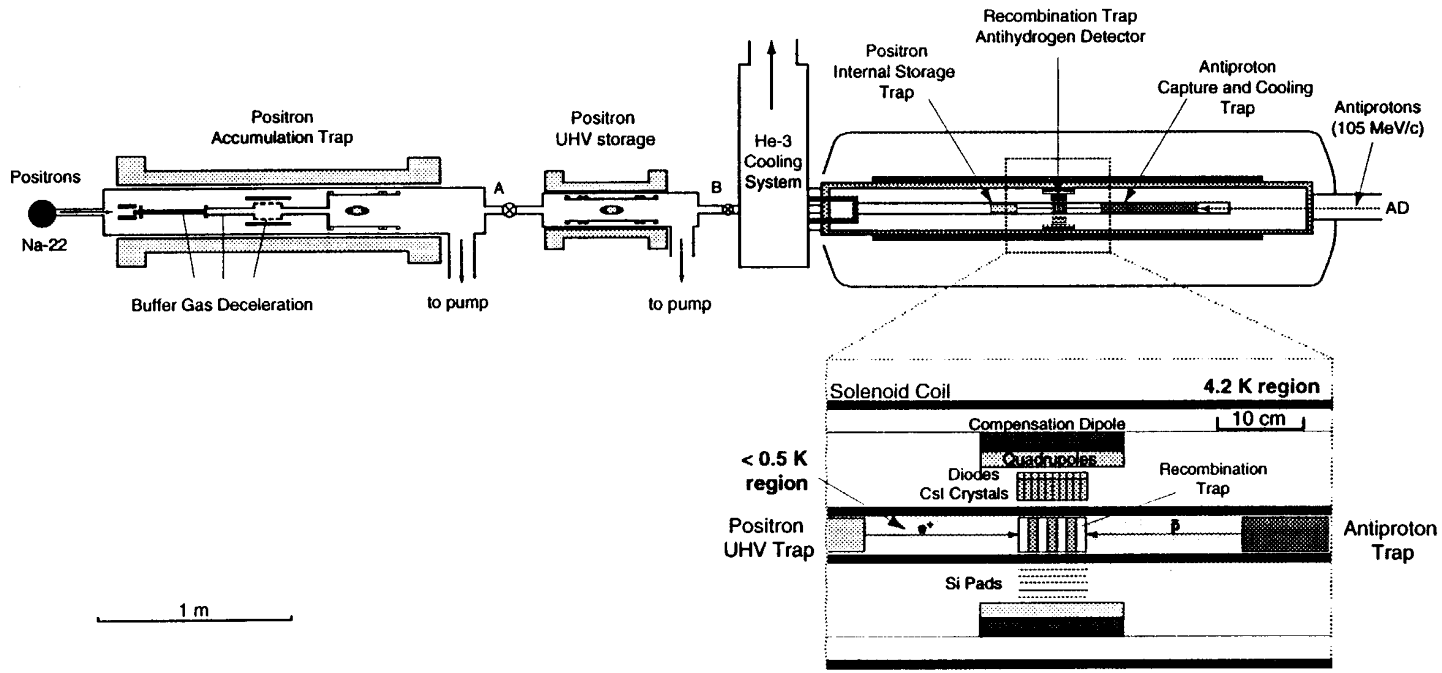

Figure 1: *Overview of the ATHENA apparatus showing the superconducting solenoid with the antiproton capture trap, the positron storage trap, and the recombination trap surrounded by the magnetic gradient trap.*

good vacuum within the cryogenic environment, the lifetime of cooled antiprotons reaches several hours or even months [37].

After the antiprotons have been cooled and stored in the central region of the trap, the capture potential at the entrance and exit electrodes can be switched off without losing antiprotons. Therefore it is possible to repeat the capture and cooling procedure several times, and both experiments have shown that this "stacking" allows increasing the number of stored antiprotons by a factor 10 or more. The enhancement figure was essentially limited by the number of LEAR shots obtainable without refilling the machine, and is expected to be much higher at the future AD, where many more pulses can be delivered to the experiments with a repetition rate of 1 pulse every 1 - 2 minutes.

3.2 Capture and cooling of antiprotons in ATHENA

The geometry of the ATHENA (ApparaTus for High precision Experiments on Neutral Antimatter) capture and cooling trap will be similar to the PS200 trap. It will be housed in a large bore solenoid (inner diameter ≥ 25 cm) with a homogeneous magnetic field ($\Delta B/B \leq 10^{-4}$) of about 3 Tesla over a 1.5 m long section. The inside of the bore is at a temperature of 4 K. The trap structure is further contained within a separate vacuum enclosure, which also accommodates the neutral (antihydrogen) trap and the internal positron storage trap. This enclosure is held at a temperature of 0.5 K or below and is completely separated from the magnet isolation vacuum and the outside by thin windows allowing injection of antiprotons and positrons. While antiprotons easily penetrate through several μ of Mylar, ultra-thin windows of less than several hundred Å must be used for positron injection. It has been shown [38] that for very low pressures, relative pressure differentials of 10^{-4} can be achieved using such foils, which in conjunction with the fast valves will be sufficient to achieve the necessary low pressure. Owing to the very good vacuum ($p \leq 10^{-17}$ Torr) which can be reached with such a completely sealed cryogenic system [37,39], it is expected that very few antiprotons annihilate during a typical experimental cycle time of about 1 hour. A ^{3}He dilution refrigerator (or an evaporative cooler) is used to reduce the temperature of the central trap structures to T = 0.5 K or below.

The incoming antiprotons traverse a beam counter, which is used for monitoring their number and the beam profile, and for triggering the high voltage switch at the entrance electrode. The AD will deliver 10^7 antiprotons per bunch, with a repetition rate of about 1 per minute. Assuming a capture efficiency of $\sim 1\%$, 10^5 antiprotons could be trapped and cooled via electron cooling to cryogenic temperatures between two AD cycles. In order to reach the nominal goal of 10^7 cooled antiprotons, about 100 AD shots would have to be stacked in the trap. However, it also appears possible to stack antiprotons from several subsequent production cycles in the AD [40], giving potentially 10^8 antiprotons per bunch, with a repetition rate of less than 6 minutes. This scheme would then only require the stacking of about 10 AD shots.

The cooling of the antiprotons will use the well-known techniques developed at LEAR. A harmonic well in the middle of the trap is pre-loaded with $\approx 10^9$ electrons, which will reach thermal equilibrium with the 0.5 K environment via synchrotron damping within a few seconds at the magnetic field to be used. The standard method to monitor the number of electrons or antiprotons is by observing the modification of the noise resonance of an RLC circuit attached to one of the central electrodes of the harmonic trap region [41]. The density of the electron and antiproton clouds in the center of the trap can be controlled by using the technique of "sideband cooling" [42].

Once a sufficient number of antiprotons (i.e. 10^7) has been accumulated and cooled, these may be transferred from the catching trap to the neutral trap. Both traps being situated inside a common solenoidal field, the transfer will be very efficient, since the problem of transporting very low energy antiprotons through magnetic fringe fields is not an issue. The temperature of the antiproton cloud will also not be affected during the transfer, provided the applied DC voltages have a stability of 0.1 mV or better.

4 Positron production and accumulation

Controlled sources of low energy positrons, and their efficient conversion to positronium atoms in vacuum, are readily available (for reviews see e.g. [43,44]). Positrons emitted from radioactive sources, or in pair production from bremsstrahlung, usually have a wide range of kinetic energies in the MeV region and upon penetrating solid matter slow typically within a few picoseconds to an energy close to the thermal level. Once slowed the positron is free to diffuse in the medium (in which most annihilate), with a diffusion length around $10^3 - 10^4$ Å and dependent upon the moderating material. During the diffusion process a positron may encounter again the surface of the solid and be spontaneously emitted into the surrounding vacuum as a free positron, or bound to an electron as positronium. Comparing the penetration depth of the positron with its diffusion length immediately gives some idea of the efficiency of moderation (i.e. the production efficiency of slow positrons in vacuum from an initially energetic ensemble incident upon the material). This is around 10^{-3} for positrons from a radioactive source, but is typically lower for the more energetic positrons from pair production.

Once the positrons have been liberated into vacuum they can easily be manipulated to form beams. Typical applications use beams with kinetic energies in the eV to tens of keV range [44]. Whether a radioactive source or an instrument which relies upon pair-produced positrons (e.g. a compact electron accelerator such as a 100 MeV microtron) is used, typical beam intensities are in the range $10^6 - 10^8$ e^+/s. When low energy positrons are incident upon surfaces in vacuum they can be re-emitted as positrons or positronium atoms under conditions which can be controlled to suit the particular experiment. Emission efficiencies can be high, even approaching 100% for positronium emission from some heated surfaces (Ref. [44] and references therein), since the positron implantation depth can be much less than its diffusion length.

In order to facilitate the production of antihydrogen by any of the schemes outlined in section 5, and its observation, it is preferable to have a pulsed positron or positronium source. This will involve the construction of a dedicated positron source and accumulator. A number of methods have been used to achieve this from radioactive source-based beams, as summarized in [44]. These include the electronic damping technique [45–47] currently being pursued by the ATRAP collaboration and the buffer gas moderating scheme of Surko and co-workers [48,49].

The latter method is by far the most efficient yet devised, and in this collaboration we propose to use a variant of this technique that incorporates accumulation under UHV conditions [50]. The basic scheme has been refined over a number of years in a series of experiments that has investigated a variety of topics including positron-matter interactions [51–54] and plasma physics [55,56]. The trapping of the positrons is effected using an axial magnetic field for radial confinement and a system of appropriately biased electrodes which form a potential well for axial confinement. The source of slow positrons is a ^{22}Na radioactive source and a solid neon moderator [57] optimized for the positron accumulator. The neon moderator, which is grown at 8 K under computer control, is capable of providing a slow positron beam flux of 2×10^7 e^+/s from a 150 mCi (5.6 GBq) source [58]

Positrons from the beam are injected into the trap over a potential hill where they interact with the N_2 buffer gas. Around 30% of the positrons lose sufficient kinetic energy to become trapped. Using the solid neon moderated primary beam, a capture rate of 55,000 e^+/s per mCi of radioactive source has been achieved [58], as compared with only a few positrons per mCi for the electronic damping method [46, 47]. The buffer gas trapping technique has achieved in excess of 10^8 positrons trapped in a vacuum of 5×10^{-10} Torr in a three minute cycle.

With modest changes the buffer gas method can be further improved to allow accumulation of 10^{10} positrons per hour [50]. We note that this estimate is conservative , since it is based upon the efficiency of our present source. DuPont Pharma now reports typical source efficiencies that are larger by a factor of four. In order to achieve this, efficient differential pumping will be employed, along with the addition of a final UHV storage stage. A schematic illustration of the set-up is shown in figure 2. The trapping sequence for the antihydrogen experiment has been described elsewhere [50]. It involves loading the trapping stage until equilibrium between the loading and annihilation rates is achieved, pumping out this stage to 5×10^{-10} Torr within one minute and then opening valve B for a short period to allow the positrons to be transferred to the storage stage.

An additional ultra-thin foil will be introduced at the entrance to the cryogenic section of the storage trap to avoid gas loading of the extreme high vacuum. Such foils typically have transmission efficiencies of $\sim$ 30%. Both the rapid pump down of the system (7 seconds per decade of pressure) and the transfer of positrons between various stages of the present accumulator have already been demonstrated experimentally [49].

The design of the new positron trap is based on the accumulated operating experience gained over the past ten years and will incorporate a number of new features to improve the performance of the device. The most important of these is an advanced internal cryo-pumping system that is being designed in collaboration with APD Cryogenics. The differential pumping will be optimized using a Monte Carlo pumping code developed by Sandia Laboratories. These improvements are expected to result in a much more compact device that uses a single magnet rather than the

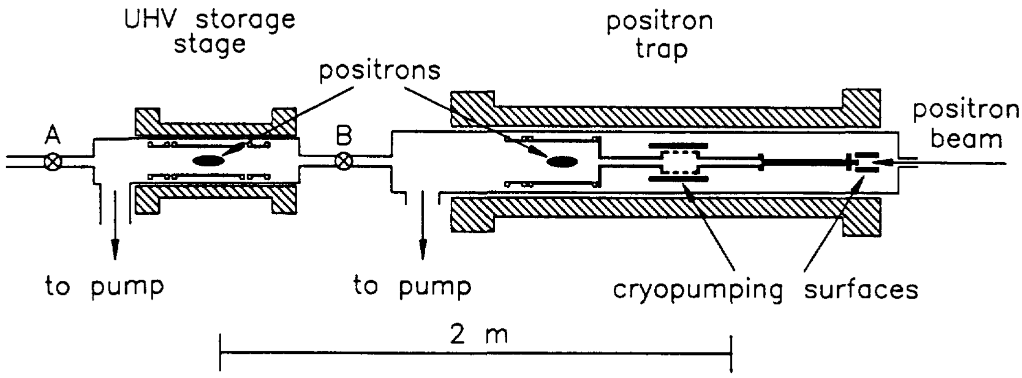

Figure 2: *Schematic illustration of a positron accumulator with ultra-high vacuum storage stage. In the actual apparatus the trapping section has three stages.*

two-magnet system presently being employed. Methods have been developed to measure *in situ* the temperature, density, and shape of the positron cloud, by monitoring the modes of oscillation of the positron plasma [49]. Given the advanced state of the development of the accumulation technique and the fact that virtually all aspects of the design for the positron accumulator have now been tested, we are confident that we can have it in place and operational at CERN by the beginning of the 1999 beam time.

Another method of accumulating low energy positrons is currently being developed by members of our collaboration and is based on the 100 MeV electron microtron at the University of Aarhus, Denmark [59]. This instrument is capable of producing around 10^6 positrons per second in 10 bunches, each about 10 μs wide. These bunches can be injected directly into an UHV storage trap as will be demonstrated at Aarhus. Several of the techniques developed for this work are of interest to the ATHENA program.

5 Antihydrogen formation

5.1 Introduction

The initial focus of the ATHENA experiment is on the production and storage of antihydrogen atoms at very low energies. The recombination technique used in the ATHENA experiment should

- provide sufficient numbers of antihydrogen atoms for spectroscopy,
- produce the atoms at very low temperatures (T $\leq$ 1 K) to allow trapping within achievable magnetic well depths,
- form antihydrogen atoms in the ground state or in low lying excited states, and
- achieve above within a reasonably short time period.

Although a technique combining all these features has not yet been demonstrated, recent experimental results have been encouraging. In addition, measurements of recombination rates of protons and electrons in storage rings and experiments with crossed beams of protons and positronium give an experimental input to check the theoretical understanding of the recombination processes.

To form a bound state of antiproton and positron starting from free particles, excess energy and momentum has to be carried away by a third particle. Various schemes for producing antihydrogen have been proposed and discussed in some detail [61–67], with the first mentioning of the possible production of antihydrogen in traps by Dehmelt and co-workers [68].

The simplest process is spontaneous radiative recombination:

$$e^+ + \overline{p} \Rightarrow \overline{H} + h\nu \tag{1}$$

(see references [60,61]). The rate for this process can be increased by laser stimulation [62]:

$$e^+ + \overline{p} + nh\nu \Rightarrow \overline{H} + (n-1)h\nu \ . \tag{2}$$

A different approach is based on three-body collisions [28]:

$$e^+ + e^+ + \overline{p} \Rightarrow \overline{H} + e^+ \ . \tag{3}$$

The above reactions require that two plasmas of opposite charge (antiprotons and positrons) are trapped and brought into contact. Alternatively, recombination by crossing a beam of positronium (either in the ground state or in low-lying excited states) with antiprotons has been proposed:

$$Ps + \overline{p} \Rightarrow \overline{H} + e^- \ , \tag{4}$$

(see references [63,64]), and

$$Ps^* + \overline{p} \Rightarrow \overline{H^*} + e^- \ , \tag{5}$$

(see references [65,66]).

In the following we discuss the basic principles of radiative and three-body recombination. Afterwards, the advantages and disadvantages of the proposed reactions are compared. In the absence of a proven scheme, we intend to pursue more than one route to trapped antihydrogen, with particular emphasis on the laser-stimulated recombination in nested traps and on the positronium-collision method.

5.2 Radiative recombination of positrons and antiprotons

Recombination between ions and electrons is an important issue in storage rings with electron cooling, since it causes significant beam losses. The measured rates of recombination, depending on the relative longitudinal and transverse velocity distributions of the two plasmas, can be used to estimate the corresponding rates in traps by considering the co-moving center-of-mass system of the ion (proton) beam.

The critical issues are the recombination rate and the initial state of the formed antihydrogen atom. Two processes are typically considered, spontaneous radiative recombination (SRR), and three-body recombination (TBR).

5.2.1 Spontaneous radiative recombination

The cross-section for spontaneous radiative recombination (SRR) [69] is related by time-reversal invariance to photo-ionization, and depends only on the kinetic energy E of the electron in the center-of-mass (c.m.) system of the proton, and the capture level n:

$$\sigma_{RR}(n, E) = 2.1 \cdot 10^{-22} cm^2 \frac{1}{nx(1+n^2x)} \tag{6}$$

$$x = E/E_0, \quad E_0 = 13.6eV, \quad E = \frac{1}{2}mv^2 \; . \tag{7}$$

The cross-section decreases with high n. The total cross-section is obtained by summing over all n up to a "cut-off" level n_{cut}, which is reached when antihydrogen atoms are ionized in collisions with neighboring atoms (E $\sim$ kT) or by external electric fields. For example, an antihydrogen atom in an n = 200 state is ionized by electric fields of about 1 V/cm or by collisions with 0.34 meV kinetic energy. Typical cross-sections are $5 \cdot 10^{-21}$ ($E_{c.m.}$ $\sim$1 eV), $1.2 \cdot 10^{-18}$ ($E_{c.m.}$ $\sim$10 meV), and $1.5 \cdot 10^{-16}$ cm^2 ($E_{c.m.}$ $\sim$ 0.1 meV). Per antiproton, the radiative recombination rate is given by the phase space overlap between electrons and protons

$$R = \int_r \int_v n_e(\vec{r}) n_p(\vec{r}) \sigma(v) v f(\vec{v}) d^3v d^3r \; , \tag{8}$$

where $n_e(r)$ and $n_p(r)$ are the spatial densities of electrons and protons, respectively, $\sigma(v)$ is the velocity-dependent cross-section for radiative recombination, and f(v) is the distribution function of relative velocities between protons and electrons. For overlapping beams with relative velocity v_r, the "recombination" coefficient α is defined as:

$$\alpha(v_r) = \int \sigma(v) v f(v_r, \bar{v}) d^3v \; , \tag{9}$$

and the recombination rate becomes :

$$R(v_r) = \alpha(v_r) \int_{vol} n_e(\vec{r}) n_p(\vec{r}) d^3r \ . \tag{10}$$

To get an order of magnitude for $\alpha(v_r)$, we consider the simple case where all velocities are equal:

$$\alpha(v_r) = \langle \sigma(v) v \rangle = \begin{cases} 3.2 \cdot 10^{-13} & cm^3 s^{-1} \ (1eV) \\ 7.1 \cdot 10^{-12} & (10meV) \\ 0.9 \cdot 10^{-10} & (0.1meV) \end{cases} \tag{11}$$

These values agree within a factor 2 or better with more elaborate calculations [70]. At the Test Storage Ring (TSR) in Heidelberg, the recombination rate measured for electron beam temperatures corresponding to $T_{\|} = 0.5$ meV and $T_{\perp} = 0.1$ eV is $1.92 \cdot 10^{-12}$ cm^3s^{-1} [71], in excellent agreement with the theoretical value of $1.93 \cdot 10^{-12}$ cm^3s^{-1}, derived from a more general calculation taking into account the asymmetric velocity distributions parallel and transverse to the beam direction [72].

To find the rates for spontaneous recombination in a nested Penning trap, we have to make some assumptions about the relative velocity distributions of the electron and the proton cloud and the spatial overlap of their distribution functions. A systematic study of these quantities by molecular dynamics simulations is being undertaken within the collaboration, but only preliminary results have been obtained so far. However, an upper limit for recombination rates can be obtained by assuming a complete overlap of proton and electron clouds, characterized by an average relative velocity v_r:

$$R(v_r) = \alpha(v_r) \int_{vol} n_e(\vec{r}) n_p(\vec{r}) d^3r \quad \sim \quad \alpha(v_r) N_e N_p / V \tag{12}$$

with $V \sim 1$ cm^3.

With $N_e = 10^6$, $N_p = 10^5$, and using the approximate value of α(v) in (11), the upper limits for the spontaneous recombination rates at different electron energies are: R = 0.03 s^{-1} (1 eV), 0.7 s^{-1} (10 meV), 9 s^{-1} (0.1 meV). Using a higher number of (anti)protons and electrons (positrons), (e.g. $N_{e^+} = 10^8$, $N_{\bar{p}} = 10^7$), these rates increase proportionally, giving an upper limit of

$$R = 300 s^{-1} (1eV), \quad 7000 s^{-1} (10meV), \quad \text{and} \quad 90.000 s^{-1} (0.1meV) \tag{13}$$

respectively. Of course, these results must be corrected for the actual overlap of the clouds.

5.2.2 Laser-induced radiative recombination

The rate for spontaneous radiative recombination is small since the emission of a photon, necessary to conserve energy and momentum, is a slow process on the time scale of a collision. Therefore laser-induced recombination (see reaction (2) and reference [62]) was proposed, in which the capture rate in particular n−states would be increased by illuminating the reaction region with photons of appropriate energy $h\nu$ corresponding to the particular continuum to bound-state transition. Laser-stimulated recombination of protons with electrons in continuum states has been studied extensively at storage rings, and has been discussed in several papers [73]. A measure for the efficiency of laser-stimulated recombination is the ratio of the induced recombination rate to the total spontaneous recombination rate, the enhancement factor G:

$$\mathrm{G}_{nl}(E_{cm}) = \frac{R_{nl}^{ind}(E_{cm})}{R_{nl}^{spon}(E_{cm})} \; . \tag{14}$$

For a maximum enhancement factor, a low energy spread in the electron (positron) energy distribution and a high laser power density are most important. The limiting effect is photo-ionization of the produced (anti)hydrogen atoms, leading to saturation of the enhancement factor when the laser intensity is increased. At the TSR in Heidelberg, proton-electron recombination into n=2 has been studied at laser pulse intensities close to 20 $\mathrm{MW/cm^2}$, leading to an enhancement factor G = 70 ± 2, not far from the expected enhancement factor of 85 [74]. A different experiment used a 15 W continuous CO_2 laser with an intensity of $\sim$ 1 $\mathrm{kW/cm^2}$ to induce transitions into n=11 , observing an enhancement factor of about ten [75].

In summary, the use of laser stimulation allows enhancement of the recombination rates by one to two orders of magnitude, depending on the laser intensity, the overlap of the laser beams with the plasmas, and the number of (anti)hydrogen atoms in high-n Rydberg states.

5.2.3 Three-body recombination in dense positron plasmas

This mechanism, where three particles (two positrons and an antiproton) collide simultaneously, only plays a role at high positron densities and low temperatures. The rate for three-body recombination $\alpha_{TBR}(n)$ as a function of the capture level n has been calculated [76] by considering the time-reversed process, i.e. electron-impact ionization of hydrogen, which is well known:

$$\alpha_{TBR}(n) = 1.96 \cdot 10^{-29} cm^6 s^{-1} n_e \left(\frac{1}{kT/eV}\right) n^6 \tag{15}$$

The steep dependence on the principal quantum number n indicates that mostly very high Rydberg states close to the "cut-off" level $n^* \sim \sqrt{R/2kT}$, $R = 13.6$ eV, are populated. Summing up all contributions from n=1 to n^*, the total three-body recombination rate for a Maxwellian positron velocity distribution of temperature T becomes:

$$\alpha_{TBR}(n^*) = 2.8 \cdot 10^{-30} cm^6 s^{-1} n_e \left(\frac{1}{kT/eV}\right)(n^*)^7 = 2.7 \cdot 10^{-27} cm^6 s^{-1} n_e \left(\frac{1}{kT/eV}\right)^{4.5} \quad (16)$$

This formula is in excellent agreement with previously quoted results [77]. A comparison with the recombination coefficient for radiative recombination shows that for positron densities $n_e = 10^6$ cm^{-3} three-body recombination becomes comparable at $kT \sim 10$ meV, and then increases by 4.5 orders of magnitude per factor 10 of decreasing temperature. Consequently, at very low temperatures this process is expected to dominate completely. Hence, a dynamic equilibrium will be reached, with as many antihydrogen atoms forming in high-n as are destroyed by collisions or field ionization. Only if an effective deexcitation mechanism is used to induce transitions to lower lying states, which then decay rapidly to the ground state, will this process be useful for the purpose of this experiment. The positrons captured in high-lying bound levels can be stabilized by stimulating a transition to lower levels, i.e. the 11.1 μm light of a $^{13}CO_2$ laser could be used to drive a transition to n = 11.

5.3 Antihydrogen production using trapped plasmas

5.3.1 Nested traps

Two plasmas of opposite charge may be stored in nested Penning traps [28]. The nested trap is an outer potential well for antiprotons, within which an inverted well for positrons is nested, with the wells being generated by applying potentials to cylindrical ring electrodes. The positrons will cool by synchrotron radiation to the ambient temperature and, provided the two plasmas overlap, the cold positron gas will cool the antiprotons by Coulomb interaction. Recently, electron cooling of protons in a nested Penning trap has been reported [47], demonstrating that: (a) particles of opposite charge can indeed be simultaneously trapped, and (b) protons get into contact with cold electrons at low relative velocity and cool down to an energy corresponding to the electron well depth. However, the observed width of the proton energy distribution (few eV) does not correspond to the thermal distribution of the electrons at 4.2 K, and has yet to be understood. Also, no recombination of electrons and protons into hydrogen has been observed to date. The latter fact may be explained by the difficulty of observing the signature of the formation of a few hydrogen atoms, which consists of detecting the disappearance of the equivalent number of protons. This task will be facilitated by studying the charge-conjugate reaction with antiprotons and positrons at LEAR, since the signature of annihilating antihydrogen can be detected with an efficiency close to 1. Such a test is foreseen in December 1996 at LEAR by the PS196/ATRAP collaboration [78], and the results will be of great interest in planning our initial experimental program.

The rate constant for this process is strongly temperature dependent ($\approx T^{-9/2}$, see above), and therefore benefits vastly from cooling the particles. The theoretical rate for extended plasmas in complete overlap is very large at 4.2 K (with a positron density of $10^7/cm^3$ positron the reaction rate becomes $\Gamma = 6 \times 10^6$ /s). However, the strong n^6 dependence of the cross-section results in a complete dominance of antihydrogen atom formation in highly excited Rydberg states (n $\geq$ 50-100) which have a long lifetime with respect to radiative deexcitation. Therefore, this method probably has to be used in combination with laser stimulation, which populates lower lying n-states before the antihydrogen is ionized by electromagnetic fields or by collisions.

5.3.2 Combined Penning and Paul traps

An alternative way to trap plasmas of opposite sign is to use a combined Penning and RF-trap (Paul trap). Such a trap employs a homogeneous static magnetic field and a static electric quadrupole field for ion confinement (Penning trap). For electrons, the repelling force from the electrostatic field is overcome by a radio-frequency-quadrupole field (Paul trap), and positrons and antiprotons can be kept in the same volume for an indefinitely long time. This arrangement was first discussed by Chun-Sing and Schüssler [79] for the capture of ions in flight. Further theoretical and experimental investigations of such a system were performed by Bate *et al.* [80]. The possibility to use such a system for the formation of antihydrogen was first mentioned by Guo-Zhong Li and G. Werth [81] who analyzed the regions of stability for particles with vastly different charge-to-mass ratios (e^- and $^{238}U^{92+}$).

Such a trap has recently been demonstrated [29] to hold several thousand electrons and protons simultaneously at estimated densities of 10^7 cm^{-3}, which is about $1/100^{th}$ of the space charge limit.

The disadvantage of this method is the heating of the electron plasma by the microwave driving force in a Paul trap, which is eventually transferred to the ions (or protons). For antihydrogen formation, this would lead to unacceptably high positron energies of the order of 0.1 eV, thus reducing the antihydrogen formation rates to rather small values. The challenge here is to reduce the microwave heating to achieve cryogenic temperatures of the particles, while keeping the positron and antiproton cloud confined.

We plan to conduct a series of laboratory test experiments to evaluate these two scenarios. The key issues to be investigated are the density, the temperature, and the overlap of the clouds achievable in the two trap configurations.

5.4 Positronium-antiproton collisions

Collisions between antiprotons and positronium atoms (reactions 4 and 5) have also been proposed as a possible recombination scheme [64], [30].The relevant cross-section can be derived from the related process of positronium formation in positron-atomic hydrogen collisions. A summary of calculations and data has been recently given by Ermolaev [82]. He stresses that recent calculations [83] have found cross-sections for antihydrogen formation of 10^{-15} cm^2 for positronium impact energies of a few electron-volts. The assumption was made that the cooled antiprotons can be treated as stationary. The calculations also show that antihydrogen is produced mostly in the ground or first excited state, given that the positronium is in its ground state.

It was pointed out some time ago [65] that the use of excited state positronium atoms for antihydrogen production (reaction 5) had some advantages over the use of the ground state. Notably, the cross-section was argued to follow a classical area scaling law (proportional to the fourth power of the positronium principal quantum number) and is therefore expected be much enhanced. (This has been supported by quantum mechanical calculations [83].) Again the antihydrogen is formed into relatively low-lying states such that, as argued by Deutch *et al.* [66], the recoil energy of the excited antihydrogen can be low.

In initial experiments, however, it is the ground state positronium which must be used. We note that the charge conjugate of reaction 4, namely hydrogen production from proton-positronium collisions, has recently been observed by members of our collaboration in an experiment based at the University of Aarhus [84,85]. The observed rates ($8.1 \pm 3.1 \times 10^{-4} \mathrm{s}^{-1}$) were in excellent agreement with theoretical predictions for the used beam intensities and energies. This, together with the detailed theoretical understanding of the reaction, means that the formation rate and the antihydrogen recoil conditions can be predicted with some confidence, given the knowledge of the antiproton and positronium spatial and velocity distributions.

An estimate of the rate of antihydrogen formation, $R_{\bar{H}}$, can be obtained from [86],

$$R_{\bar{H}} = 4N_{\bar{p}}\sigma_H \epsilon I(\tan^{-1}(r/d)^2)/\pi^3 r^2 \tag{17}$$

where $N_{\bar{p}}$ is the number of stored antiprotons (taken to be 10^7), σ_H is the formation cross-section ($10^{-15} cm^{-2}$), ϵ is the positronium formation efficiency at the selected surface (taken to be 0.2), and r and d are the radius of the antiproton cloud and its distance from the positronium source respectively, each assumed to be around 5mm. The positron intensity, I, is assumed to be 10^{10} [50], delivered in a burst from the last stage of the positron accumulator which was described in section 4. Inserting values we obtain $R_{\bar{H}} \approx 10$ per hour, i.e. ten for each accumulation of 10^{10} positrons.

A Monte Carlo simulation of the antihydrogen production from reaction 4 has also been carried out. Inputs to this program are the distributions of electron recoil angles for various positronium kinetic energies [83] and the positronium energy distribution itself. For our calculations we use those distributions found for an aluminum surface at a cryogenic temperature and bombarded by 50 eV positrons. They overlap both the maximum in σ_H and the positronium kinetic energy at which the minimum recoil energy for 1S antihydrogen is expected. The simulation was carried out at the two antiproton temperatures of 4.2 and 0.5 K, with the antiproton velocity distribution taken to be a Maxwell-Boltzmann at each temperature. The results so far suggest that only around 1% of the antihydrogen is produced with a recoil temperature at, or below, the expected depth of the neutral magnetic trap of 1 K when the antiproton temperature is 4.2 K. This is antihydrogen in the 1S state which forms around 30%

of the time , with the remainder being formed approximately 5% in the 2S state, 40% in the 2P state and the remaining 25% in higher states. In addition, the simulation reveals that the antihydrogen does not recoil isotropically. The excited states are produced mostly in a distribution about the direction of the incident positronium, as is the ground state for high incident positronium energies. At low energies, however, the 1S antihydrogen recoils preferentially in the opposite direction. Such behavior may prove of value for the initial detection of the antihydrogen, or for experiments where separation of the formed atoms from the trap region should be desirable.

We consider this method as being worthwhile to pursue in order to produce antihydrogen. However, very few antihydrogen atoms will be eventually captured in the magnetic trap. At present, the expected rates for this mechanism are too low for spectroscopic measurements. However, a careful study of enhancing the cross-sections and lowering the recoil momentum by using excited positronium atoms may change these conclusions.

6 Magnetic traps for antihydrogen

Having discussed the generation, trapping of all necessary components, and possible recombination schemes whereby antihydrogen can be formed, the next task is to combine all this into an environment suitable for trapping and studying the neutral antihydrogen atoms. Much of the development work in this area will be guided by the excellent work of the groups at MIT [87, 88], and Amsterdam [89], who have developed the technology to magnetically confine dense clouds of hydrogen atoms.

Here, the force exerted by the magnetic gradient onto the magnetic moment of the neutral atoms is used for confinement. This separates the (anti-)hydrogen into low-field seeking and high-field seeking atoms. Even though work with hydrogen has been performed with both species, only the low-field seeking states are of use in the case of antihydrogen, where collisions with the walls of the containment vessel are unacceptable. The trap configuration used for the latter case normally consists of an arrangement of coils, designed to produce a magnetic minimum at the center of the trap without having a zero field location, which would introduce spin-depolarizing Majorana transitions. The essentially cylindrical geometry of these traps in the Ioffe-Pritchard configuration [32] provides transverse trapping forces by a set of superconducting race track coils which generate a quadrupole field. Axial confinement is typically achieved through coaxial solenoids at either end of the trapping volume, which provide a barrier against axial leakage and also the non-zero field value in the center. Ioffe-Pritchard magnetic traps have been successfully used by members of our collaboration in their research with hydrogen at MIT [90] as well as by the group in Amsterdam [91]. Typically trap depths of 1K were achieved with magnet currents of 100 A.

The proposed static magnetic trap for the ATHENA apparatus is a modified version of the Ioffe-Pritchard configuration designed with the goal of achieving the highest possible trap depth while allowing room for the particle detection system and the antiproton trap. In our apparatus the trap consists of four superconducting race-track "quadrupole" coils and one solenoid (compensation solenoid) running oppositely to the main solenoid to generate a field minimum in axial direction. We propose to mount the compensation solenoid and the quadrupole coils to the inside of the superconducting solenoid of the main magnet system, where they can be cooled by the cryogenics of this section. This lay-out is schematically shown in figures 1 (side-view) and 3 (cross-section). Using typical values for current densities in the superconducting coils, this design will generate a well depth sufficient to confine neutral atoms with a kinetic energy below 0.5 K.

A good knowledge of the field inside and outside the trap region is required to understand the dynamics of the antihydrogen atoms captured as well as for particle tracking. These field calculations have been done, and are being continuously refined, using the ANSYS code package at CERN [92]. Once the final configuration has been decided upon, these data will be available to be used for simulations of the detection efficiency by the particle detection group in the ATHENA collaboration.

When working with hydrogen, magnetic traps are filled by allowing the hydrogen "gas" to fall into the potential well by inelastic collisions with residual gas atoms and the walls, a method unacceptable for antihydrogen. Therefore we propose to superimpose the magnetic trap onto the Penning and/or combined trap to be used for the recombination process in such a way that the antihydrogen formation takes place in the minimum of the magnetic well. Antihydrogen produced in the high-field seeking states will quickly leave the trap volume, while the low-field seeking states would be repelled by the magnetic barrier and, if the well depth is higher than the kinetic energy of the formed atoms, would be trapped.

One complication of this approach which must be studied carefully is the question of possible instabilities of charged particle clouds of high density in an azimuthally non-symmetric magnetic field [93]. It has been observed that dense electron clouds in elongated Penning-type traps exhibit a short life-time due to misalignments of the magnetic and electrical axes of the experiment [94]. No information exists on the strength of this loss-mechanism in three dimensional, harmonic Penning traps. Therefore part of our collaboration plans to perform tests on this effect using the positron accumulator at the University of California at San Diego.

7 Detection of Antihydrogen

The goal of the detector surrounding the antihydrogen trap is to discriminate between the annihilation of antihydrogen on one side, and the separate annihilation of antiprotons and positrons on the other side, to reconstruct the annihilation vertex with good resolution, and to provide high rate capabilities to study the evolution in time of the recombination process and rate.

The detector consists of two parts: one part concerns the detection of charged particles stemming from the annihilation of an antiproton with matter in or around the recombination trap. The second part concerns the detection of the two back-to-back 511 keV γ's from e^+e^- annihilation. For the best detection efficiency, the detector must be positioned as close as possible to the recombination trap, and cover as large as possible a solid angle without interfering with other priorities (magnetic trap, laser system).

This requires that the detector be placed inside the superconducting solenoid, which is at a temperature of 4 K. In order to be able to use commercially available detector and electronics components, the detector will have to be placed in a thermally insulated and temperature regulated enclosure. This enclosure consists of an outer enclosure at 4 K, surrounding an inner enclosure maintained at a higher temperature. The two enclosures are isolated from each other by several layers of aluminized mylar. To minimize thermal radiation from the inner to the outer enclosure, and possibly into the recombination trap region, the temperature of the inner enclosure is chosen to be as low as possible, but high enough to allow the functioning of all electronic components. The exact temperature must be determined in lab tests, but will lie at or below 70 K, since both types of detectors, as well as the read-out electronics, are known to work at this temperature [95,96].

The lay-out of the detector is shown in Fig. 3. The volume outside of the trap and inside of the quadrupole coils houses four stacks of silicon pad detectors (SPDs) on opposite sides of the recombination trap for charged tracking and vertex determination, and four blocks of CsI crystals (for detection of the two 511 keV γ's), also on opposite sides of the trap, but rotated by 45° with respect to the SPDs. The four-fold symmetry is chosen for physics reasons (back-to-back γ's), but also for modularity, access and simple reconfiguration. In particular, individual modules can be removed and be replaced by i.e. Lyman-α sensitive detectors at a later stage.

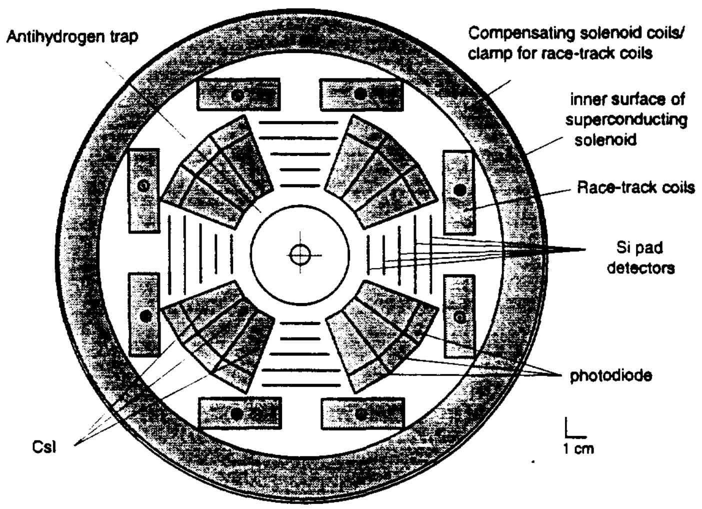

Figure 3: *Transverse view of the detector.*

7.1 Charged particle detection

Antiproton-matter annihilation at rest produces several charged particles , with momenta around 300 MeV/c. These charged particles must first traverse the trap electrodes, the walls of the inner dewar, the wall of the surrounding vacuum vessel, and finally the walls of the enclosure of the detectors. Multiple scattering in these layers leads to an uncertainty of the annihilation vertex position of about 1 mm. The accuracy of the hit measurement in each of the five layers of the SPD should be matched to this extrapolation accuracy.

The SPD stacks consist of 5 layers of silicon pad detectors. The two innermost layers have dimensions 2×8 cm^2, the next layer has dimensions 3×8 cm^2, and the outermost two layers have dimensions 4×8 cm^2. Each layer consists of several smaller modules of dimensions 1×4 cm^2, read out at one end, containing 128 pads of dimensions 1.25 mm (transverse) $\times$ 2.56 mm (in the z-direction). The thickness of each detector is 1 mm. Multiple scattering is not an issue with the achievable coordinate measurement precision, and such a large thickness improves the signal-to-background ratio and has the added advantage of decreasing the detector capacitance for the backplane read-out. Thinner prototype detectors with 256 pads of 2 x 2 mm^2 have been tested [97,98] and give an excellent signal-to-noise ratio of 80:1 at room temperature, which should even improve at lower temperatures. Fig. 4 shows the signals for minimum ionizing particles (mips) as seen by the prototype detector.

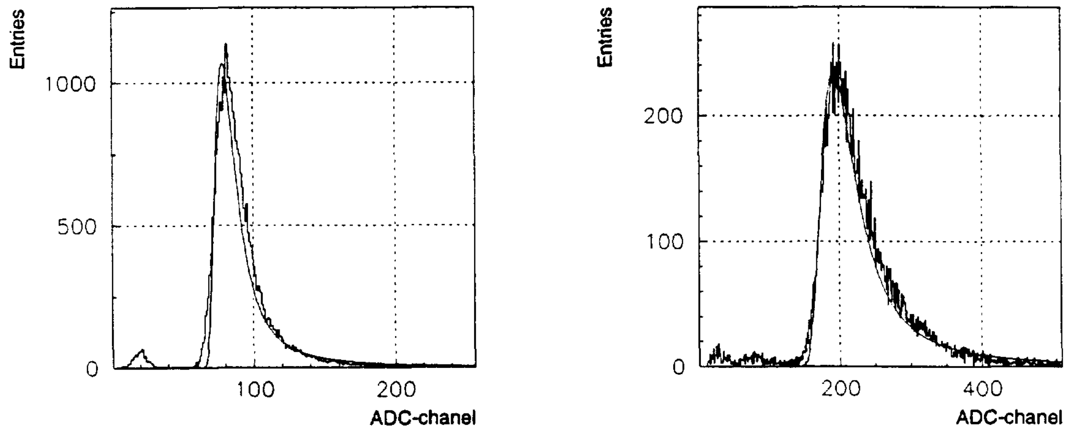

Figure 4: *Landau spectra for minimum ionizing particles as seen by the back plane (left) and by the pads (right plot) of a prototype detector.*

The 128 pads of each silicon pad detector are read out via a VA1 preamplifier chip [99]. This chip consists of 128 sample-and-hold elements in parallel, followed by a preamplifier and is read out serially at 5 MHz. Fifteen VA1's are daisy-chained to read out one half of one stack in about 400 μs. Signals from the VA1's are fed into ADC's (CAEN C-RAMS with a memory depth of 2048 channels). Pedestal subtraction and zero suppression are performed in this unit; the remaining data is then read into the memory of the data acquisition computer (DAQ) before being written to storage.

For triggering purposes, this standard read-out system of the individual silicon pad detectors is supplemented by a second independent system based on the back-plane read-out currently used by the Crystal Barrel experiment [100]. Measurements with prototype detectors [98] give a signal-to-noise for back-plane read-out of about 10:1, and show a clear correlation between signals measured on the pad side of a detector and those independently measured on the back plane of the same detector (Fig. 4). With its time resolution of $\sim$ 100 ns, the back-plane readout not only allows triggering at rates up to 10^7 events/s, but also permits charged particle reconstruction (albeit at a ten times worse resolution than the pad readout) with each 1×4 cm^2 detector element functioning as a single large pad.

7.2 511 keV γ detection

Tagging of e^+e^- annihilation requires detection of two 511 keV γ's in coincidence and in a back-to-back geometry. The electromagnetic calorimeter is a 10 cm long cylinder which lies at a radial distance of 4 cm and consists of 120 crystals of pure CsI with dimensions 1x1x3 cm^3. Good results have been obtained with crystals of pure CsI at low temperatures. The total light output increases strongly with decreasing temperature (Fig. 5), requiring precise temperature control of the calorimeter enclosure. This is accompanied by a shift of the emission spectrum towards longer wavelengths which are better suited to detection by photodiodes.

The granularity of the calorimeter allows the position determination of two interacting 511 keV γ's - and thus of the production (annihilation) point - to approximately 1 cm. The solid angle covered by the calorimeter is approximately 50% of 4π, while the conversion probability for a 511 keV γ in 3 cm CsI is about 80%, leading to a total detection efficiency for simultaneous detection of both γ's of about 30%. The effective efficiency for the tagging of two 511 keV γ's is reduced with respect to this upper limit by requiring the signals to lie clearly above the noise; this is easily achievable if the 511 keV γ's interact via the photoelectric effect, but more difficult if either or both Compton scatter, and thus deposit a fraction of their energy in neighboring crystals. Separation of minimum ionizing particles from 511 keV γ's is straightforward since the former deposit 16.7 MeV in 3 cm CsI. A similar argument holds for photons produced from neutral mesons from $\bar{p}p$ annihilation.

The presence of a strong, inhomogeneous magnetic field requires the use of photodiodes for the readout of the scintillation light. Many steps, most of them dealing with crystal preparation, are necessary to ensure that sufficient light can be collected to allow using a photodiode rather than a photomultiplier [101]. A further critical element is the matching of the crystal and photodiode surfaces. We plan on using a Hamamatsu S3590 photodiode which has a sensitivity higher than that of conventional types. In the case of 3 cm long crystals the ratio of covered surface to available surface is 57%. A 5 mm light guide will thus be glued to the outside end of the crystals to reduce the cross-section to the active area of the photodiode of 1 x 1 cm^2.

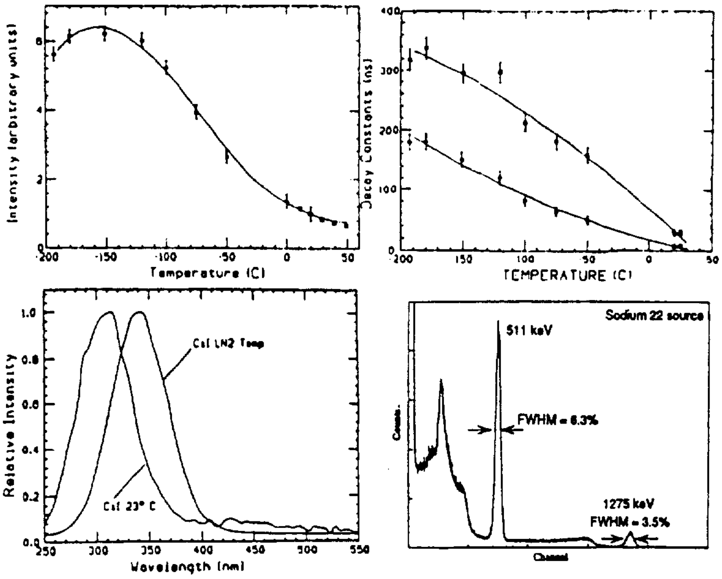

Figure 5: *Variation in the light intensity of the fast light output (top left) and in the decay constants (top right) of the two fast components in undoped CsI as a function of temperature. Bottom left: emission spectrum of undoped CsI at 23* deg*Celsius and at liquid Nitrogen temperatures. Bottom right:* ^{22}Na *spectrum for a 1* cm^3 *CsI(Tl) crystal read out with a Hamamatsu 3590 photodiode.*

The resolution of a properly prepared CsI crystal read-out via such a scheme (Fig. 5) shows that the photopeak can be clearly separated from the noise, and that the obtained resolution rivals that of photomultipliers.

7.3 Trigger and performance

Given the rather low recombination rates to be expected, the initial trigger can be relatively loose. Should background rates turn out to be a problem, further (topological) cuts are easily implemented. Two triggers will run in parallel, i.e. either one will trigger a read-out of the full detector. The first ("charged") trigger consists of a signal seen in at least three SPD backplanes. A similar trigger is presently being used in the Crystal Barrel experiment [100]. The second ("neutral") trigger consists of requiring a signal above the noise in at least two crystals. The efficiency of the neutral trigger depends critically on the light output of the crystals and on the performance of the photodiodes; if necessary, a trigger with lower efficiency but higher selectivity could be constructed by requiring the signals in two crystals to be consistent with the photopeak. With these two triggers, it is possible to record $\bar{H}$ annihilations, as well as $\bar{p}$ annihilations or e^+ annihilations separately. Instantaneous annihilation rates up to 10^7 s^{-1} with the SPDs and up to 10^5 s^{-1} with the CsI calorimeter are resolvable.

Each crystal of the calorimeter will be calibrated in the lab with sources to establish linearity and response. In situ, the 511 keV line from positron annihilation will be used to calibrate the individual crystals and the detector as a whole.

The SPD towers will be assembled around the neutral trap before installation, and their position will be measured in the lab. The support structure of the four towers will assure their relative alignment to 0.1 mm. Distortions due to temperature changes will be determined in the lab or in a test beam. The determination of the absolute position of the detector relative to the neutral trap will be possible by reconstructing the annihilation vertices of a large number of $\bar{p}$ annihilations on the trap walls.

8 Laser systems for antihydrogen

Production, cooling, and spectroscopy of antihydrogen may require three distinctly different laser systems at various stages of the experimental program. The first stage of the experiment will be devoted to producing large numbers of antihydrogen atoms, capturing them at kinetic energies corresponding to the magnetic well depth, and performing spectroscopic measurements with a precision limited by the Zeeman broadening under these conditions. This part of the program requires a 243 nm laser source with very small line width for 1S-2S spectroscopy, and (possibly) a laser system to stimulate recombination. At a later stage, the linewidth of the 1S-2S transition can be reduced by laser cooling of antihydrogen. This will require a number of developments which are discussed below.

8.1 Antihydrogen spectroscopy

The main goal of our experimental program, the high precision spectroscopy of antihydrogen, will require the construction of an intense, stable light source at 243 nm with very small line width. A number of groups have advanced the technology over the last years [90, 102], and we will be able to build on the existing experience and technology. In a typical system this light is produced by doubling the frequency of a ring dye laser, which is pumped by a Krypton-Ion laser, and is stabilized to an external optical resonator via a radio-frequency sideband modulation technique. The stability of this reference cavity is crucial for the experiment, and much care must be taken to achieve the highest possible finesse and the best possible mechanical isolation from the surroundings. Currently the best stability achieved is about 1 kHz at 486 nm. The light output from the ring dye laser is then doubled in a nonlinear BBO crystal, and a few tens of milliwatt can be generated using a standing wave resonator. As an indication, 100 mW of circulating power and a beam waist radius of 0.4 mm would yield the necessary light intensity for reaching the initial goals of our experiment. Recently, the generation of light at 243 nm using an all solid state laser system [103] has been demonstrated.

8.2 Recombination

A detailed discussion of laser-stimulated recombination to form antihydrogen atoms has been given elsewhere [104], and we summarize only the salient points. With respect to spontaneous radiative recombination, rate enhancements by 1-2 orders of magnitude by laser stimulation have been demonstrated [74, 75]. For three-body recombination, the effect of the stimulated transitions is to connect the high Rydberg levels, which have a small probability of spontaneous radiative decay, to the low-lying levels with a high spontaneous decay rate. The final stabilization is effected by the spontaneous decay of the low-lying level. For recombination at rest, transitions from the near-continuum states to the 11D level of antihydrogen could be induced by a $^{13}C^{16}O_2$ infrared laser wavelength of $\sim$ 11.1 μm. As a possible option, a second laser at a wavelength of $\sim$ 377 nm may be used to induce 11D-2P transitions. Such a two-step scheme has the advantage of requiring a smaller laser saturation intensity than a one-step scheme.

8.3 Laser cooling

The ultimate precision in antihydrogen spectroscopy - given by the natural 1S-2S line width (1.3 Hz) - can only be achieved by cooling the antihydrogen atoms to the lowest possible temperatures. Also, measurable gravitational effects only appear for kinetic energies of antihydrogen in the milli-Kelvin range, since the difference in gravitational potential for a change in height of 1 meter is equivalent to the kinetic energy of an antihydrogen atom at 1 mK. At present, laser cooling appears to be the most promising technology. For antihydrogen, it is prohibitive to thermalize by collisions with cryogenic walls because of the expected loss from annihilation. Evaporative cooling relies on the thermalization via collisions between antihydrogen atoms, but the expected collision rates are too low at the anticipated antihydrogen densities.

The kinetic energy of antihydrogen atoms at formation is close to the average kinetic energy of the antiproton cloud before recombination. By thermal contact with a dilution refrigerator, a temperature of the antiprotons of 50-100 mK can be reached. The very low initial temperature of the produced antihydrogen thus avoids the very challenging task of using laser cooling starting at the temperature of liquid He (4.2 K), which would require much higher Lyman-α intensities than presently available.

Laser cooling of hydrogen atoms in one dimension is achieved by exciting e.g. a 1S-2P transition via absorption of Lyman-α photons from a laser beam. The subsequent spontaneous emission with the decay time of the 2P level (1.6 ns) is isotropic, so that a dissipative force acts on the hydrogen atom slowing it down along the axis defined by the laser beam. This technique has been demonstrated for cooling of hydrogen atoms from 80 mK to 8 mK, which is only a factor 3 higher than the Doppler limit (2.4 mK) [105]. However, hydrogen cooling in three dimensions was obtained by relying on collisions within a dense sample of atoms, which is not an option for antihydrogen.

The need for cooling antihydrogen in three dimensions without relying on collisions in a dense sample of atoms requires the use of more powerful Lyman-α light sources. The principal technological problem is that 122 nm is in the vacuum ultraviolet (VUV) region, where no nonlinear crystals or laser oscillators are available. Therefore, the light must be produced by frequency mixing in gases. Various schemes are being investigated: a) tripling of 365 nm UV radiation in a phase-matched Krypton-Argon gas mixture [106,107], b) two-fold doubling of 851 nm produced in a Nd:YAG pumped dye-laser to produce light at 212 nm, which is then focused into a mixing cell containing Krypton (for Lyman-α generation) and Argon (for phase matching) [108,109], c) frequency doubling of 243 nm in atomic hydrogen under an external electric field [110]. The latter method would have the advantage of allowing the use of the same 243 nm source needed for antihydrogen spectroscopy.

9 Physics experiments with antihydrogen

9.1 High resolution spectroscopy of antihydrogen

A central goal of the ATHENA collaboration is to compare the level structure of antihydrogen with that of hydrogen with the highest possible precision. The most interesting spectroscopy is the two-photon 1S-2S transition at the excitation wavelength of 243 nm, half the Lyman-α frequency, with a natural linewidth of 1.3 Hz. This linewidth represents an accuracy of 5 parts in 10^{16}, which, with a sufficiently high signal-to-noise ratio, could be enhanced to 1 part in 10^{18} by determining the line center to high accuracy.

Doppler-free two-photon spectroscopy was first proposed by Chebotaev [111] in the early 70's, and first demonstrated by the group of T. W. Hänsch at Stanford University. Atoms are excited by two counter-propagating light fields at 243 nm, whose first-order Doppler shifts cancel. The excited 2S atoms are detected via the emission of Lyman-α photons or by photoionization. Since there is no nearby intermediate resonance state, such an experiment requires intense and highly monochromatic light sources, which became available only in the mid 1980's. In 1989, Boshier *et al.* [112] took advantage of the then newly commercially available crystal material BBO, which permits efficient doubling of the blue 486 nm light from a dye-laser. At this time the experiments were for the first time no longer limited by the laser bandwidth, but by collisional and transit time broadening of the sample gas cell.

The next generation of experiments was initiated by the group of T. W. Hänsch in Munich [113], using a cold atomic beam traveling collinear to the standing wave light field. Now the accuracy was limited by the second-order Doppler effect due to the velocity of the atoms, and by actively selecting the low velocity component of the beam. The narrowest line achieved with this method so far has been about 3 kHz wide, representing a relative accuracy of 2.8 $\times 10^{-12}$ [114]. At MIT, a record relative resolution of 2 parts in 10^{12} with a high signal-to-noise ratio in this transition has recently been achieved [115] by using cold, trapped hydrogen atoms.

The typical detectors used for observing L_α fluorescence from the excited hydrogen atoms in these experiments are microchannel plates (MCPs). Using a CsI coating on the input face of the MCP, quantum efficiencies of 25% can be reached. It has been shown that MCPs can be operated without a significant loss of efficiency at 4 K temperatures and in high magnetic fields, provided the input rate is kept low [116]. Such an MCP detector can be implemented into our set-up at a later stage, possibly replacing one of the quadrants of the particle detector. The solid angle of such a detector can be maximized with the use of light pipes, either at L_α or at a down-converted frequency.

The currently achieved resolution is again limited by laser frequency instabilities and the lack of a good reference standard to which the laser frequency can be locked. Additionally, for conversion of this resolution into an absolute precision of a frequency measurement, improvements in the current frequency standards, as well as in the comparison of UV light to such standards, is necessary. Possibly the best method to minimize systematic shifts and to achieve the highest precision in the hydrogen-antihydrogen comparison is to use trapped hydrogen atoms to provide the reference frequency to which the laser can be locked. The apparatus currently used by the MIT and Amsterdam hydrogen groups is rather elaborate, since there the main goal is to produce an ultra-cold, extremely dense atom sample to observe Bose-Einstein condensation. For the purpose of providing a frequency reference for our experiment, one does not need to achieve quite as low a temperature and by far not as high a density, and we anticipate that a simpler apparatus will suffice.

Laser spectroscopy of antihydrogen will require in many respects a rather different technology from what has been used so far with hydrogen. Experiments will have to be carried out in the comparatively harsh environment of an accelerator. The first improvement would be the replacement of the sensitive dye laser system by a frequency doubled Ti:Sapphire laser, operating at 972 nm. In the future it may become possible to start with a high power diode laser at 972 nm, eliminating the need for large Ar^+ or Kr^+ ion pump lasers. A similar development will be necessary in terms of providing a smaller and more robust hydrogen frequency standard.

An additional complication in performing spectroscopic experiments on trapped antihydrogen is the relatively small number of atoms available. Unlike in beam experiments, where a continuous stream of hydrogen atoms can be used, or in the trapped hydrogen experiments at MIT in dense samples, most efficient use of the antihydrogen atoms is required. The excitation of atoms to the 2S level is detected through field-induced Lyman-α fluorescence. Both the quenching field and the spontaneous L_α emission will cause spin flips and cause the atoms to leave the trap. This can be avoided by using a microwave transition to cycle the atom through the $2P_{3/2}, F = 2, m = 2$ state, ensuring that the atom always decays back into the low-field seeking ground state. Additionally, the power available in the VUV light necessary to excite the 1S-2S transition may cause photo-ionization of the n=2 level, representing a potentially much more serious loss mechanism. Zimmermann [117] estimates the number of atoms needed for high-resolution spectroscopy. By balancing the need for minimizing the photo-ionization losses by a fast quenching rate against the unavoidable line broadening introduced by quenching, he estimates that with 1000 atoms at 0.2 K a fractional accuracy in determining the center of the line would be better than 1 part in 10^{12}, if the Zeeman-broadening and the quench-broadening are both kept at about 20 kHz.

Achieving such an accuracy is the immediate goal of our collaboration. It exceeds the currently available CPT tests of the electromagnetic interaction by 2 orders of magnitude. Further improvements appear feasible, in principle up to the theoretical limit of the natural linewidth, but will require many further technical developments, including efficient laser cooling of antihydrogen atoms in the trap. This will be the subject of continuing efforts of the ATHENA collaboration.

9.2 Gravity studies on antimatter

If spectroscopic comparisons of antihydrogen to hydrogen would yield a difference, this would not necessarily constitute a violation of CPT, but could also be interpreted as an anomalous red-shift of the antiatom. Hughes [118] has studied the consequence of an anomalous gravitational coupling to antimatter, with a range larger than the distance of the Earth to the Sun, but smaller than our galaxy. Assuming exact CPT symmetry and a tensor force gravitational interaction with infinite range, he showed that a comparative measurement of the 1S-2S transition frequency in hydrogen and antihydrogen at a level of 1 part in 10^{15} would test the weak equivalence principle for positrons at a level of 1 part in 10^{11}. Such tests are not model-independent and would require a variety of further experiments to distinguish between possible violations of CPT or the weak equivalence principle. Therefore, direct measurements would be preferable and would yield valuable complementary information, albeit with lower precision.

Several ideas for experiments of this type are being discussed within our collaboration and are being analyzed for their possible merit. The main problem to be faced is that at a temperature of 3 mK, which is close to the Doppler-limit for laser cooling, a cloud of antihydrogen atoms will be distributed vertically in the gravitational potential over a height of ≈ 2.5 meter. Similarly, a free falling cloud of antihydrogen at this temperature would expand due to its internal temperature much faster than it would fall due to the gravitational acceleration. Despite these problems, initial studies indicate that a precision of a few percent or better may be achieved with such methods.

It has been discussed [119] that, assuming the availability of a horizontal beam of about 4000 antihydrogen atoms with a velocity of about 10^4 m/s, an interferometric technique as demonstrated with sodium atoms by Pritchard's group [120] could yield a measurement of the gravitational acceleration of antihydrogen at a level of 1%. Potentially a much more powerful, but also much more elaborate, method would be a derivation of the atom interferometer developed by S. Chu in Stanford [121]. Using an atomic fountain of sodium atoms he used consecutive Raman transition pulses with well defined phase and duration to split and then recombine the atomic wave function while rising in the gravitational field. The final state depends on the phase difference between the two arms of the interferometer which is linearly dependent on the gravitational acceleration "g". A sensitivity to gravity at the level of 1 part in 10^8 was quoted for the measurements on sodium, and an accuracy of 10^{-10} was predicted if the (heavier and therefore slower) cesium atom would be used.

All these experiments will need laser cooling to the lowest possible temperature and each of them will require a specific trap design, different from the one presently planned for ATHENA. Therefore none of these ideas can be directly incorporated into the ATHENA physics program. Nevertheless, the scientific potential of such studies is recognized and a detailed analysis of possible scenarios will be pursued in parallel to the development of the source of ultra-cold antihydrogen atoms by part of our collaboration.

9.3 Other experiments with ultra-cold antiprotons

Experiments with extremely low energy antiprotons are of continuing interest. It has been discussed on several occasions that such experiments would profit from using a catching trap similar to that currently being used in PS200.

It has been decided by the ATHENA collaboration that none of these ideas can be incorporated into the ATHENA program without compromising our primary goals. Instead we suggest that an independent group form around the original PS200 catching trap to address implementation of such a program. A separate proposal to the SPSLC describing the technical aspects of such a program and discussing the different physics questions which can be addressed by such an apparatus, is currently being prepared.

Possible experiments include:

(a) Collision studies with ultra-low energy antiprotons .
(b) Stored antiprotons for biological and medical applications.
(c) Nuclear density distribution measurements.
(d) Formation of exotic atoms in pbar-H collisions.
(e) Heating of plasmas by antiproton annihilation.
(f) Capture of antiprotons into metastable states in helium .
(g) Gravity studies with ultra-cold antiprotons.

10 Floor space and infrastructure

We request an area of approximately 7 meter wide and 25 meter long for the installation of our experimental apparatus. This area will need to accommodate (a) the final section of the beam line transporting the antiproton pulse from the AD to our experimental zone (including beam monitoring equipment), (b) the main section of the ATHENA apparatus as shown in figure 1 with the antiproton capture trap, the recombination section, and the positron storage trap, (c) the positron accumulator described in section 4, and (d) some of the support structure for the superconducting magnet (i.e. transfer or buffer dewar for liquid helium, gas handling system and control panel for dilution refrigerator, etc.). Additionally, space is needed for the installation of the laser systems for stimulated recombination, 1S -2S spectroscopy, and for the later addition of laser cooling. These laser systems must be mounted with the maximum amount of vibration isolation. We anticipate to elevate the laser system above floor level to allow continuous access to the systems during AD operation. Nevertheless, the underlying floor space must be reserved for a solid base for this installation and will not be accessible to other equipment. Figure 6 shows a schematic lay-out of the experiment in the AD hall.

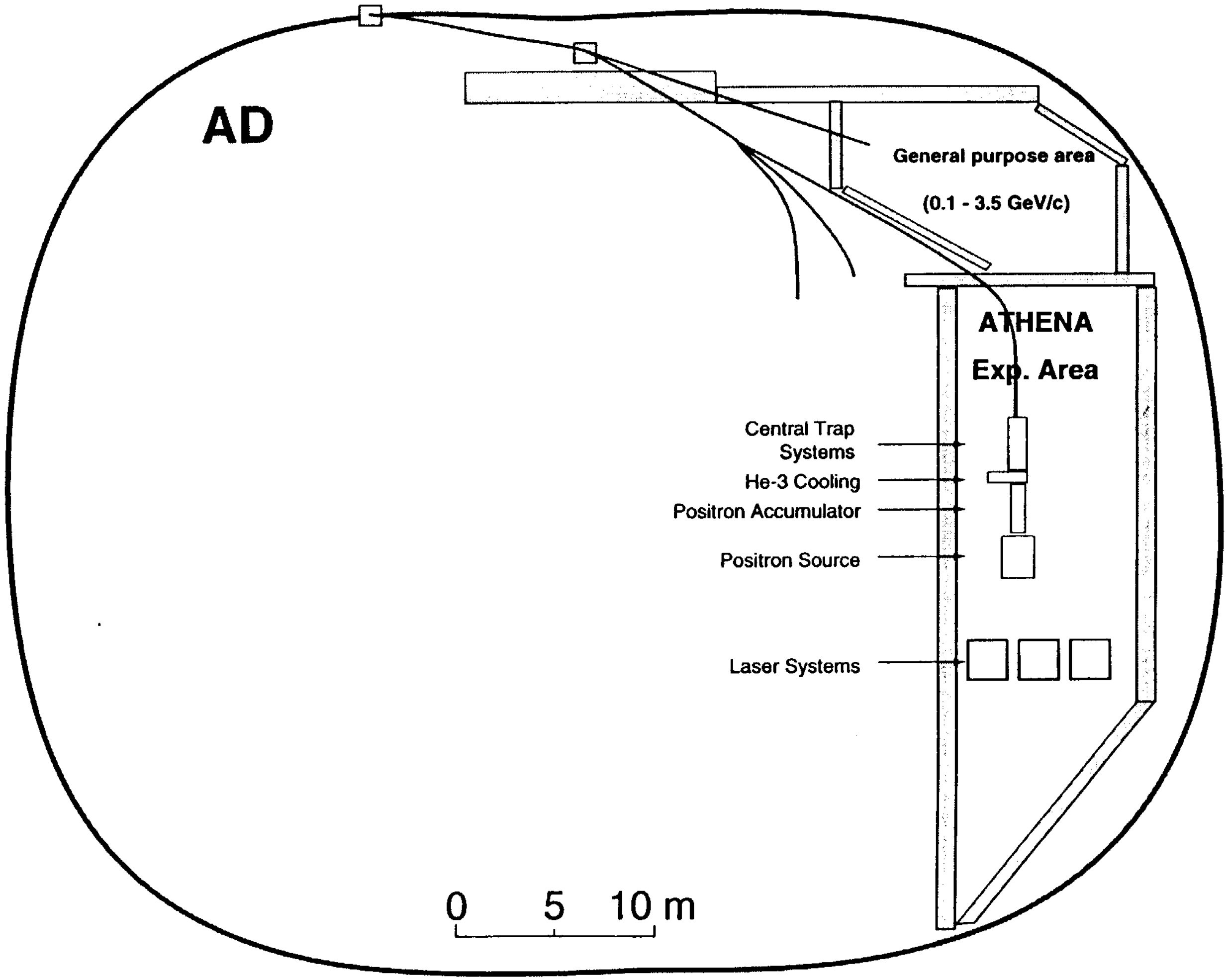

Figure 6: *General lay-out of the ATHENA apparatus on the floor of the AD experimental area*

In addition to this experimental floor space we request adequate space for remote installation of the data acquisition and slow control systems.

The experiment will require both 220 Volt single phase and 380 Volt three phase power lines to be brought into the zone. These power lines should be separated from the accelerator system and should have noise filters installed at the entrance to the zone or the electronics area. We will need a standard supply of gaseous helium and nitrogen as support for the cryogenic systems, and iso-butane and SF_6 supplies for beam counters and energy fine tuning in a similar amount as currently being used at PS200 at LEAR.

To supply the cryogenic systems of the main solenoid as well as the dilution refrigerator with liquid helium we propose to install a liquefier system, which can be used jointly by all experiments, directly into the AD hall. For the dilution refrigeration system a pumping station occupying roughly 30 m^2 of floor space is required. Because of the mechanical vibration of these pumps it is requested that a room adjacent to the AD hall is made available for this installation.

Appendix I: Cost Estimate

	Description	KCHF
1	Large Bore Superconducting Magnet System	1,300
2	Dilution Refrigerator with Support Systems	1,000
3	Antiproton Catching Trap	250
4	Positron Accumulator	350
5	Laboratory Test Equipment	300
6	Magnetic Trap	250
7	Antihydrogen Detector	
	(a) Charged Particles	150
	(b) Gamma Detection	200
8	DAQ and Slow Control	200
9	Laser Systems and Optics	650
10	Hydrogen Reference System	100
	Total	**4,750**

Appendix II: Experimental plans and milestones

1997 Design and construction of individual components.

(a) Development of the positron accumulator.
(b) Construction of the antiproton catching trap.
(c) Design of the magnetic trap.
(d) Studies of different recombination methods.
(e) Construction of the antihydrogen detector.

1998 Installation and test of key elements at the AD site.

(a) Installation and commissioning of the ATHENA trap system and antihydrogen detector.
(b) First capture and cooling of antiprotons from the AD.

1999 Production of Antihydrogen

(a) Stacking of antiprotons, accumulating $\geq 10^7$ antiprotons in the trap.
(b) Installation and tests of the positron accumulator.
(c) First formation and detection of low energy antihydrogen.

2000+ Spectroscopy of antihydrogen.

(a) Collection of antihydrogen in magnetic gradient trap.
(b) Spectroscopy of antihydrogen (1S-2S transition).
(c) Study laser cooling of antihydrogen in magnetic trap.
(d) Gravitational studies

References

[1] G. Lüders, Kong. Danske Vidensk. Selsk. Mat.-Fys. Medd. 28 No. 5 (1954) 1; Ann. Phys. 2 (1957) 1.

[2] W. Pauli, in: *Niels Bohr and the Development of Physics*, ed. by W. Pauli (Pergamon, New York, 1955), p. 30.

[3] J. S. Bell, Proc. Roy. Soc. A 231 (1955) 479.

[4] R. Jost, Helv. Phys. Acta 30 (1957) 409; *The General Theory of Quantized Fields* (American Mathematical Society, Providence, Rhode Island, 1965).

[5] J. J. Sakurai, *Invariance Principles and Elementary Particles* (Princeton University Press, Princeton, 1964); R. F. Streater and A. S. Wightman, *PCT, Spin & Statistics, and All That* (Benjamin, New York, 1964).

[6] Particle Data Group, Phys. Lett. B204 (1988) 46

[7] R. S. Van Dyck, P. B. Schwinberg, and H. G. Dehmelt, Phys. Rev. Lett. 59 (1987) 26.

[8] G. Gabrielse, D. Phillips, W. Quint, H. Kalinowsky, and G. Rouleau, Phys. Rev. Lett. 74 (1995) 3544.

[9] A. Kostelecky and R. Potting; report IUHET 236, hep-th/9211116

[10] P. Huet and M. Peskin; Nucl. Phys. B434 (1995) 3

[11] A. Kostelecky and R. Potting; Phys. Rev. D51 (1995) 3923

[12] D. Colladay and A. Kostelecky; Phys. Lett. B344 (1995) 259;

[13] J. Ellis, J. Lopez, N. Mavromatos and D. Nanopoulos, CERN-TH.95-99;

[14] D. Colladay and A. Kostelecky; Phys. Rev. D 52 (1995) 6224

[15] R. Adler *et al.* (CPLEAR) and J. Ellis, J. Lopez, N. Mavromatos and D. Nanopoulos, CERN-PPE/95-149

[16] T. Prokopec, R. Brandenberger, A. Davis and M. Trodden; CLNS 95/1368, hep-ph/9511349;

[17] J. Ellis, N. Mavromatos and D. Nanopoulos, CERN-TH/96-189

[18] P. Huet; UW/PT 96-11, hep-ph/9607435;

[19] A. Kostelecky and R. van Kooten; accepted for publication in Phys. Rev. D;

[20] A. Kostelecky;Talk at PANIC '96, May 1996, hep-ph/9607482;

[21] R. M. Wald; Phys. Rev. D 21 (1980) 2742.

[22] D. H. MacIntyre and T. W. Hänsch, Metrologia 25 (1988) 61.

[23] M. Charlton, J. Eades, D. Horvath, R. J. Hughes, and C. Zimmermann, Phys. Rep. 241 (1994) 65.

[24] R. J. Hughes, M. H. Holzscheiter; Journal of Modern Optics 39 (1992) 263.

[25] M. H. Holzscheiter; Physica Scripta T59 (1995) 326

[26] S. Maury, *et al.*; CERN/PS 96-43 (AR)

[27] Guo-Zhong Li, R. Poggiani, G. Testera, G. Torelli, and G. Werth; Hyperfine Int. 76 (1993) 343

[28] G. Gabrielse, S. L. Rolston, L. Haarsma, and W. Kells; Phys. Lett. A129 (1988) 38

[29] J. Walz, S. B. Ross, C. Zimmermann, L. Ricci, M. Prevedelli, and T. W. Hänsch; Phys. Rev. Lett. 75 (1995) 18

[30] J. W. Humbertson, M. Charlton, F. M. Jacobsen, B. I. Deutch; J. Phys. At. Mol. Phys. B20 (1987) L25

[31] Y. V. Gott, M. S. Ioffe, V. G. Tel'kovskii; Nucl. Fusion, 1962 suppl., Pt. 3 (1962) 1045

[32] D. E. Pritchard; Phys. Rev. Lett. 51, 1336 (1983).

[33] G. Gabrielse, X. Fei, L. A. Orozco, R. L. Tjoelker, J. Haas, H. Kalinowsky, T. A. Trainor, W. Kells; Phys. Rev. Lett 63 (1989) 1360

[34] M. H. Holzscheiter, X. Feng, T. Goldman, N. S. P. King, R. A. Lewis, M. M. Nieto, G. A. Smith; Phys. Lett. A 214 (1996) 279

[35] M. H. Holzscheiter; Physica Scripta 46 (1992) 272

[36] G. Gabrielse, L. Haarsma, and S. L. Rolston; Int. J. Mass Spec. and Ion Processes 88 (1989) 319

[37] G. Gabrielse, X. Fei, L. A. Orozco, R. L. Tjoelker, J. Haas, H. Kalinowsky, T. A. Trainor, and W. Kells, Phys. Rev. Lett 65 (1990) 1317

[38] V. Lagomarsino, G. Manuzio, A. Pozzo, and G. Testera; Nucl. Inst. Meth. A307 (1991) 309

[39] W. Thompson and S. Hanrahan, Jour. Vac. Sci. Tech. 14 (1977) 643

[40] S. Maury, CERN, private communication (1996)

[41] X. Feng, M. Charlton, M. H. Holzscheiter, R. A. Lewis, Y. Yamazaki; J. Appl. Phys. 79 (1996) 8

[42] D. J. Wineland and H. G. Dehmelt, Intl. J. Mass Spectr. Ion Phys. 16, (1975) 338

[43] P. J. Schultz and K. G. Lynn; Rev. Mod Phys., 60 (1988) 701

[44] M. Charlton and G. Laricchia, Hyperfine Int. 76 (1993) 97

[45] P. B. Schwinberg, R. S. VanDyck and H. Dehmelt, Phys Lett **A81** (1981) 119

[46] L. Haarsma, K. Abdullah and G. Gabrielse, Phys Rev Lett 75 (1995) 806

[47] D. S. Hall, G. Gabrielse; Phys. Rev. Lett. 77 (1996) 1962

[48] T. J. Murphy, C. M. Surko; Phys. Rev. A46 (1992) 5696

[49] R. G. Greaves, M. D. Tinkle, C. M. Surko; Phys. Plasmas 1 (1994) 1439

[50] C.M. Surko, R.G. Greaves and M. Charlton, to be published in Hyperfine Int.

[51] C. M. Surko, A. Passner, M. Leventhal, and F. J. Wysocki, Phys. Rev. Lett. 61 (1988) 1831

[52] T. J. Murphy and C. M. Surko, Phys. Rev. Lett. 67 (1991) 2954

[53] S. Tang, M. D. Tinkle, R. G. Greaves, and C. M. Surko, Phys. Rev. Lett. 68 (1992) 3793

[54] K. Iwata *et al.*, Phys. Rev. A51 (1995) 473

[55] C. M. Surko, M. Leventhal, and A. Passner, Phys. Rev. Lett 62 (1989) 901

[56] R. G. Greaves, M. D. Tinkle, and C. M. Surko, Phys. Rev. Lett 74 (1995) 90

[57] A. P. Mills, Jr., and E. M. Gullikson, Appl. Phys. Lett. 49 (1996)

[58] R. G. Greaves and C. M. Surko, to be published in Can. J. Phy. (1996)

[59] J. P. Merrison and H. Knudsen, private communication

[60] G. Budker and A. Skrinsky; Sov. Phys.-Usp. 21, 277 (1978)

[61] H. Herr, D. Möhl, and A. Winnacker; in *Proc. 2nd Workshop on Physics with Cooled Low Energy Antiprotons at LEAR*, Erice, May 9-16, 1982, (eds. U. Gastaldi and R. Klapisch) p. 659, Plenum, New York 1984

[62] R. Neumann, H. Poth, A. Wolf, and A. Winnacker; Z. Phys. A313, 253 (1984)

[63] B. I. Deutch, F. M. Jacobsen, L. H. Andersen, P. Hvelplund, H. Knudsen, M. H. Holzscheiter, M. Charlton, G. Laricchia, Phys. Scrip. T22, 288 (1988)

[64] B. I. Deutch, L. H. Andersen, P. Hvelplund, F. M. Jacobsen, H. Knudsen, M. H. Holzscheiter, M. Charlton, and G. Laricchia; Hyperfine Int. 44, 271 (1988)

[65] M. Charlton; Phys. Lett. A143, 143 (1990)

[66] B. I. Deutch, M. Charlton, M. H. Holzscheiter, P. Hvelplund, L. V. Jørgensen, H. Knudsen, G. Laricchia, J. P. Merrison, and M. R. Poulsen; Hyperfine Int. 76 (1993) 153

[67] C. T. Munger, M. Mandelkern, J. Schultz, G. Zioulas, T. A. Armstrong, M. A. Hasan, R. A. Lewis, and G. A. Smith; Proposal to Fermilab (1992)

[68] H. Dehmelt, R. Van Dyck, P. Schwinberg, and G. Gabrielse; Bull. Am. Phys. Soc. 24, 757 (1979)

[69] H. A. Bethe and E. E. Salpeter; *Quantum Mechanics of One- and Two- Electron Atoms*, Springer Verlag, Berlin (1957)

[70] M. Bell, J. S. Bell, Part. Acc. 12 (1982) 49

[71] A. Wolf *et al.*, Z. Phys. D21 (1991) 69

[72] A. Wolf, in *Recombination of Atomic Ions*, eds. W. G. Graham *et al.*, NATO ASI Series B: Physics, Vol. 296, Plenum, New York, 1992; p.209

[73] A. Wolf, Hyperfine Int. 76 (1993) 189, and ref. therein

[74] U. Schramm *et al.*, Phys. Rev. Lett. 67 (1991) 22

[75] F.B. Yousif *et al.*, Phys. Rev. Lett. 67 (1991) 26

[76] M. Pajek, R. Schuch, to be published; Poster at the 2nd Euroconference on Atomic Physics with Highly Charged Ions, Stockholm, June 1996

[77] P. Mansbach, B. Keck, Phys. Rev. 181 (1969) 275

[78] G. Gabrielse, H. Kalinowsky, W. Jhe, T. W. Hänsch, C. Zimmermann, J. Walraven, T. Hijmans, W. Oelert, W. D. Phillips, S. L. Rolston, and D. Wineland; Letter of Intent SPSLC 96-23/I211 (1996)

[79] Chun-Sing O, Hans A. Schüssler; J. Appl. Phys. 52 (1981) 2601.

[80] D. J. Bate, K. Dholakia, R. C. Thompson, D. C. Wilson; J. of Mod. Optics 39 (1992) 305.

[81] Guo-Zhong Li, G. Werth; Physica Scripta 46 (1992) 587

[82] A. M. Ermolaev, to be published in Hyperfine Int. (1996)

[83] J. Mitroy and A. T. Stelbovics; J. Phys. B27 (1994) L79, and priv. comm.

[84] J. P. Merrison, H. Bluhme, J. Chevallier, B. I. Deutch, P. Hvelplund L. V. Jørgensen, H. Knudsen, M. R. Poulsen, M. Charlton and G. Laricchia; submitted to Phys. Rev. Lett. (1996)

[85] J. P. Merrison, to be published in Hyperfine Int. (1996)

[86] M. Charlton; to be published in Can. J. Phys. (1996)

[87] H. F. Hess, G. P. Kochanski, J. M. Doyle, N. Masuhara, D. Kleppner, and T. Greytak; Phys. Rev. Lett. 59, 672 (1987).

[88] D. Kleppner, in *The Hydrogen Atom*, editors: G. F. Bassani, M. Inguscio, T. W. Hänsch; Springer Verlag, Berlin (1989) p. 103

[89] J. T. M. Walraven, R. van Roijen, and T. W. Hijmans; in *The Hydrogen Atom*; eds. G. F. Bassani, M. Inguscio, and T. W. Hänsch; Springer Verlag Berlin, Heidelberg (1989); and J. T. M. Walraven; Hyperfine Int. 76 (1993) 205.

[90] C. L. Cesar, D. Fried, T. Killian, A. Polcyn, J. Sandberg, I. A. Yu, T. J. Greytak, D. Kleppner, and J. M. Doyle; Phys. Rev. Lett. 77 (1996) 255

[91] I.Setija, H.Werij, O.Luiten, M.Reynolds, T.Hijmans, J.Walraven, Phys. Rev. Lett. 70 , 2257 (1993)

[92] Luca Venturelli, priv. communication

[93] C. Surko, priv. communication

[94] C. F. Driscoll; in *Proc. of the Antimatter Facility Workshop*, Univ. of Wisconsin, Madison, October 3 - 5, 1985

[95] F. Sauli, Instrumentation in High Energy Physics, World Scientific (1992)

[96] O. Toker, IDEAS, private communication.

[97] P. Weilhammer *et al.*; CERN-PPE/96-57

[98] N. Danneberg, Diploma thesis, LMU München 1996, unpublished.

[99] O. Toker *et al.*, Nucl. Inst. Meth. A340 (1994) 572.

[100] Ch. Regenfus, to be published in Nucl. Inst. Methods (1996)

[101] A. J. Bird *et al.*, IEEE Transactions on Nuclear Science, Vol. 40, Nb. 4 (1993) 395, and S. Cherry *et al.*, IEEE Transactions on Nuclear Science, Vol. 42, Nb. 4 (1993) 1058.

[102] F. Schmidt-Kaler, D. Leibfried, M. Weitz, T. W. Hänsch; Phys. Rev. Lett. 70 (1993) 2261

[103] C. Zimmermann, J. Walz, T. W. Hänsch; Hyperfine Int. (1996) in press

[104] A. Wolf, Hyperfine Int. 76 (1993) 189

[105] I.Setija, H.Werij, O.Luiten, M.Reynolds, T.Hijmans, J.Walraven, Phys. Rev. Lett. 70 (1993) 2257

[106] H. Langer, H. Puell, and H. Röhr, Opt. Commun. 34 (1980) 137

[107] R. Hilbit and R. Wallenstein, IEEE J. Quantum Electron. QE-15 (1981) 1566

[108] W. D. Phillips, S. L. Rolston, P. D. Lett, T. McIlrath, N. Vansteenkiste, and C. I. Westbrook; Hyperfine Int. 76 (1993) 265

[109] J. Marangos *et al.*; J. Opt. Soc. Am. B7 (1990) 1254

[110] K. Hakuta, L. Marmet, and B. Stoicheff, Phys. Rev. A 45 (1992) 5152

[111] L. S. Vasilenko, V. P. Chebotaev, and A. V. Shishaev; JETP Lett. 12 (1970) 113

[112] M. G. Boshier, P. E. G. Baird, C. J. Foot, E. A. Hinds, M. D. Plimmer. D. N. Stacey, J. B. Swan, D. A. Tate, D. M. Warrington, and G. K. Woodgate; Phys. Rev. A 40 (1989) 6169

[113] M. Weitz, A. Huber, F. Schmidt-Kaler, D. Leibfried, and T. W. Hänsch; Phys. Rev. Lett. 72 (1994) 328

[114] D. Leibfried; PhD Thesis, MPI Munich, August 1995

[115] C. Cesar *et al.*, in *Proceedings of the Fifth Symposium on Frequency Standards and Metrology* ed. J. Bergquist, Cape Cod (1995) World Scientific

[116] J. A. Schecker, M. M. Schauer, K. Holzscheiter, and M. H. Holzscheiter; Nucl. Inst. Meth. A320 (1992) 556

[117] T. W. Hänsch, C. Zimmermann; Hyperfine Int. 76 (1993) 47

[118] R. J. Hughes, M. H. Holzscheiter; J. Mod. Optics 39 (1992) 263

[119] T. J. Phillips; in *Low Energy Antiproton Physics, LEAP '94*, eds. G. Kernel *et al.*; World Scientific (1995) 589

[120] D. W. Keith, C. R. Ekstrom, Q. A. Turchette, D. Pritchard; Phys. Rev. Lett. 66 (1991) 2693

[121] M. Kasevich and S. Chu, Appl. Phys. B 54 (1992) 321.